Ceramics International 44 (2018) 17447–17452

Contents lists available at ScienceDirect

Ceramics International

journal homepage: www.elsevier.com/locate/ceramint

# Effect of growth temperature on AlN thin films fabricated by atomic layer deposition

Yong Kim, Min Soo Kim, Hee Ju Yun, Sung Yeon Ryu, Byung Joon Choi*

*Department of Materials Science and Engineering, Seoul National University of Science and Technology, Seoul 01811, Republic of Korea*

ARTICLE INFO

*Keywords:*
Atomic layer deposition
Aluminum nitride
Analysis for deposited layer
Electrical property

ABSTRACT

Resistive random-access memories (RRAM) have been extensively studied because of their advantages such as low operating voltage, high reliability, and simple structure. Among the various types of materials for RRAMs, such as oxides, nitrides, sulfides, and chalcogenides, AlN shows resistive switching phenomena with low energy and high speed via the formation of Al-rich conducting channels owing to the generation of nitrogen vacancies. Moreover, AlN has a large band gap (~ 6.2 eV), high thermal conductivity, and dielectric constant. Therefore, AlN can find application as a gate dielectric material, functional layer, and resistive switching layer for RRAM applications. In this study, AlN thin film is deposited by thermal atomic layer deposition (ALD), which is a self-limiting technique through ligand exchange between the precursor molecules and surface functional groups. We use trimethylaluminum (TMA) and $NH_3$ as the metal precursor and reaction gas, respectively. We obtain growth rates of 0.05–0.16 nm/cycle at a wafer temperature of 274–335 °C. Structural and chemical properties of the AlN films grown at various temperatures are investigated by X-ray diffraction, Auger electron spectroscopy, and X-ray photoelectron spectroscopy. The electrical properties of these AlN films are studied by fabricating the devices having an Al/AlN/Pt stack.

## 1. Introduction

Recently, resistive random-access memories (RRAM) have been actively studied due to their advantages such as low operating voltage, high reliability, and simple structure [1]. Nitride materials, such as AlN, GaN, and $Si_3N_4$, exhibit resistive switching characteristics similar to oxide materials [1]. In particular, AlN is capable of low-energy and high-speed operation via the formation of Al-rich conduction channels [2]. In addition, AlN can be a useful material due to its versatile properties, for example, wide band gap (~ 6.2 eV), high melting temperature, high thermal conductivity, high dielectric constant, and good chemical stability [3,4]. By virtue of these properties, AlN has been used in gate dielectrics, passivation layers for GaN, GaAs, and SiC semiconductor devices, as well as in RRAMs [3,5–8].

AlN thin films can be prepared one of the following methods: sputtering [9], metal-organic chemical vapor deposition [10,11], plasma enhanced chemical vapor deposition [12], and molecular beam epitaxy [13]. These deposition techniques usually demand high process temperature (400–1200 °C); at high temperatures, it is difficult to achieve precise thickness control, which is needed for microelectronics application [3]. Recently, atomic layer deposition (ALD) processes have also been used for AlN film deposition [14–16]. ALD can be performed at a relatively low temperature with high uniformity [4]. ALD can also offer control of thickness down to the monolayer level based on a self-limiting reaction [17]. Further, ALD can achieve high conformality in high-aspect structures [18].

Both thermal and plasma-enhanced ALD methods have been used to grow AlN thin films [19,20]. The growth of AlN films at different growth temperatures has been studied by many research groups based on the plasma enhanced atomic layer deposition (PEALD) method [17,21]. In this study, we investigated the effect of growth temperature in AlN films by thermal ALD, and studied the growth kinetics and structural, chemical, and electrical properties of the ALD thin films at different temperatures.

## 2. Experiment

ALD was performed with a traveling wave-type chamber (CN-1, Atomic Classic, Korea). TMA (trimethylaluminum) was used as a metal precursor, $NH_3$ as a reaction gas, and $N_2$ as purge gas. TMA was carried by vapor-draw, while $NH_3$ and $N_2$ were allowed to flow at the rate of 60 and 200 sccm (standard cubic centimeters per minute), respectively. The base pressure and process pressure of the chamber were 9.6 and 800 mTorr. A bare Si substrate was used for the growth experiment.

* Corresponding author.
*E-mail address:* bjchoi@seoultech.ac.kr (B.J. Choi).

https://doi.org/10.1016/j.ceramint.2018.06.212
Received 24 March 2018; Received in revised form 7 June 2018; Accepted 25 June 2018
Available online 26 June 2018

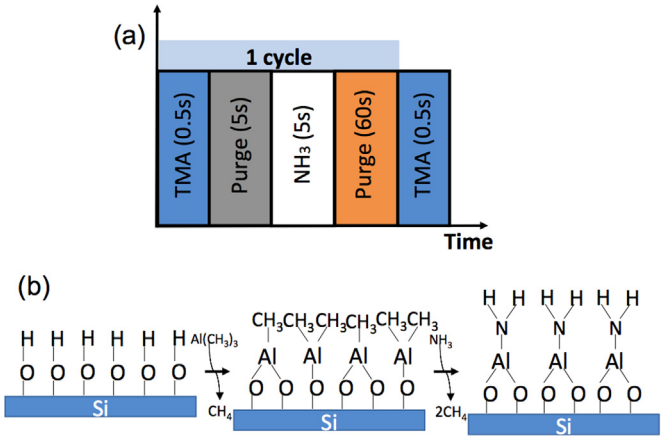


**Fig. 1.** Schematics of (a) ALD pulse sequence and (b) possible ligand exchange reaction of the ALD process.

Fig. 1(a) shows the schematic of the ALD process. The sequence of the ALD reaction consists of TMA feeding - $N_2$ purge - $NH_3$ feeding - $N_2$ purge. At first, TMA was introduced into the reaction chamber, which could react with the surface functional group (e. g. OH group) on the Si substrate. After TMA had been anchored to the substrate, the excess (unreacted) TMA was removed from the chamber by $N_2$ purge gas. Next, $NH_3$ reaction gas was introduced and reacted with adsorbed TMA precursor molecules. The by-product and the unreacted $NH_3$ were removed from the chamber by another $N_2$ purge step. ALD process cycle could be repeated until the target of film thickness is achieved. Fig. 1(b) shows the probable reaction sequence during the ALD cycle described simply above. To get the pulse time condition, self-limited growth per cycle (that is, growth rate) was acquired by increasing feeding and purge time. As a result, the pulse condition for AlN film was determined to be TMA feeding (0.5 s) - $N_2$ purge (5 s) - $NH_3$ feeding (5 s) - $N_2$ purge (60 s), as shown in Fig. 1(a). The deposition temperature ($T_{dep}$) was varied from 274° to 335°C.

The thickness of the AlN thin film was measured by a 4-wavelength ellipsometer (Film Sense, FS-1, US). X-ray diffractometry (XRD) was used to investigate the crystallinity of the film depending on the growth temperature. JEM-2100F high resolution transmission electron microscopy (TEM) at an operating voltage of 200 kV was used for the cross-sectional image of AlN film grown on Si (100) substrate. Cross-sectioning of TEM sample was performed by FEI Nova Nanolab 600 focused ion beam (FIB) with $Ga^+$ ion. Auger electron spectroscopy (AES) was used for the analysis of chemical composition. The chemical composition and bonding state in AlN film were characterized by x-ray photoelectron spectroscopy (XPS). XPS analysis was performed using a PHI 5000 Versaprobe (Ulvac-PHI) equipped with a monochrome Al Kα (1488.6 keV) source. Electrical characteristics of AlN thin films were investigated by semiconductor parameter analyzer (SPA) (Hewlett-Packard, HP-4155A, US). For the device fabrication, AlN was deposited on a 400-nm-thick Pt film on thermally grown $SiO_2$ on Si at $T_{dep}$ of 274 °C, 307 °C and 335 °C. As a top electrode, a 70-nm-thick Al film was deposited using an e-beam evaporator with shadow mask. The schematic of the device is shown in Fig. 2. The DC current ($I$) – voltage ($V$) and current density ($J$) – electric field ($E$) curve of the device were measured at room temperature.

## 3. Results and discussion

Fig. 3(a) shows the thickness of AlN thin films deposited at 274, 307, and 335 °C as a function of number of ALD cycles. At each deposition temperature, nonlinear growth was observed in the early deposition cycle, but eventually linear growth behavior was obtained. Nonlinear growth in the early cycle is related to the nucleation behavior

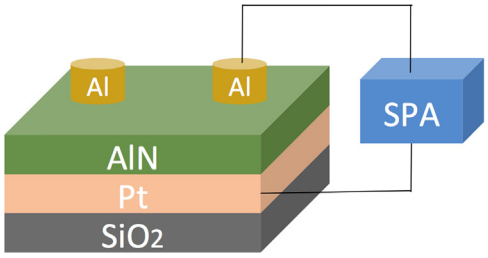


**Fig. 2.** Schematics of the device for the electrical measurement.

of the film, which is sensitive to the density of surface functional group on the substrate and its reactivity with precursors [22]. Growth rate could be obtained from the slope of the linear fitting as shown in the figure. Fig. 3(b) shows that the growth rate is increased monotonically with increasing temperature, where the growth rates are 0.02, 0.05, 0.09, 0.13, and 0.16 nm/cycle at 265, 274, 287, 307, and 335 °C, respectively. It was reported that $NH_3$ gas could react with the adsorbed TMA to form AlN at 245 °C [24]. The inset of Fig. 3(b) shows the Arrhenius plot of the growth rate as a function of $1000/T_{dep}$. From the slope of the linear fitting, the effective activation energy of AlN reaction was determined to be 55 KJ/mol (0.57 eV), similar to the reported value (0.56 eV) [20].

Strong temperature dependency on the growth rate could be explained by the low reactivity of $NH_3$ with TMA in this temperature range. H. V. Bui et al. recently reported that self-limiting growth of AlN was confirmed in the temperature range of 330–350 °C in their thermal ALD process with TMA and $NH_3$, while strong temperature dependency on the growth rate was also shown in the range of 330–370 °C [4]. Ozgit et al. [16] reported that the constant growth rate was only achieved between 100 and 200 °C by their plasma-enhanced ALD process, but not by thermal ALD with the same precursors. Therefore, the quite narrow ALD temperature window in thermal ALD process could be explained by the insufficient $NH_3$ reactivity with TMA precursor.

Dependence of growth temperature on the crystallinity of AlN films was investigated using XRD. XRD patterns of AlN thin films deposited at 274, 287, 307 and 335 °C are shown in Fig. 4(a). AlN film grown at 274 °C had an almost amorphous structure. Meanwhile, a peak at $2\theta = 33.22°$ was observed in as-grown AlN film at 287 °C, which likely originated from the wurtzite (100) plane. The intensity of the peak increases with increasing $T_{dep}$, which means that crystallinity increased as $T_{dep}$ increased. In addition, peaks from wurtzite (002) and (101) plane were detected at $2\theta = 36.04°$ and 37.92° in the film grown at 335 °C. Similar result was reported in AlN film with wurtzite crystallites grown by plasma enhanced ALD with TMA and $N_2 + H_2$ mixed gas at $T_{dep} = 350$ °C [23]. Crystallinity of AlN film was further confirmed by cross-sectional TEM analysis. Fig. 4 (b) shows cross-sectional image of 20-nm-thick AlN film on Si substrate deposited at 335 °C. Film appears to be well-crystallized to columnar structure with average grain size of ~ 3.5 nm in radius. Selected area electron diffraction (SAED) pattern is given in the inset of Fig. 4 (b).

The depth profile of the elements in the AlN films deposited at 274, 307, 335 °C was studied by AES as shown in Fig. 5(a)-(c). Uniform Al and N concentration were observed in depth while slightly N-rich film was grown under $NH_3$ reaction gas condition. High oxygen concentration was observed at the surface at all temperatures meaning that the surface oxidized when the film surface was exposed to air after deposition process. A relatively small quantity of oxygen and carbon existed in AlN films inside. Fig. 5(d) shows the average concentration of each element in the AlN thin films at the deposited temperatures. Oxygen concentration decreased remarkably with increasing $T_{dep}$, Higher deposition temperature causes crystallization of AlN film, so that crystallized film could prevent from the permeation of oxygen. When it comes to defective carbon concentration, it might be increased due to thermal decomposition of TMA as $T_{dep}$ was increased [4].

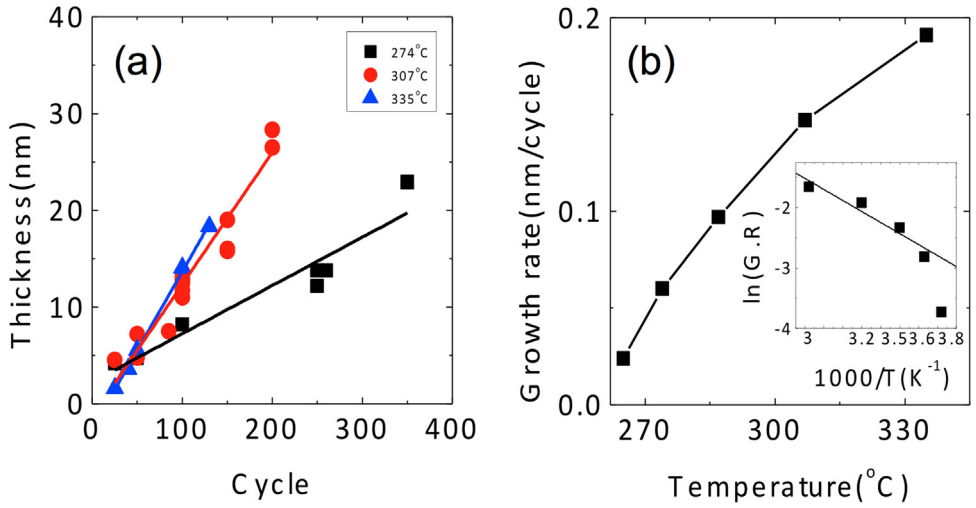


**Fig. 3.** (a) Growth per cycles of AlN thin films deposited at 274, 307, and 335 °C and (b) growth rate in the temperature range of 265–335 °C. Inset shows Arrhenius plot of growth rate and linear fitting to obtain the activation energy for the ALD reaction.

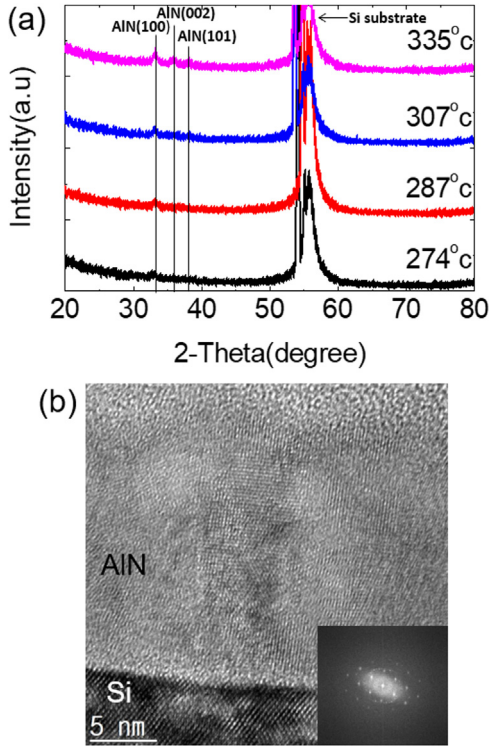


**Fig. 4.** (a) X-ray diffraction of AlN thin films in θ–2θ mode and (b) cross-sectional TEM image of AlN film grown at 335 °C (inset: selected area electron diffraction (SAED) pattern).

However, we obtained AlN films with low carbon concentration at all $T_{dep}$. This shows that AlN film was deposited not by CVD reaction of thermal decomposition but by ALD reaction of ligand exchange at all deposition temperatures in this experiment. Compared to negligible carbon content in AlN film grown by PEALD process [16], carbon was incorporated by several percent in the film by thermal ALD, similar to the previous report [4].

The chemical bonding state of elements in the AlN films were characterized by XPS. Fig. 6(a), (c), and (e) show the XPS spectra of Al 2p from AlN film grown at 274, 307 and 335 °C. The binding energies (BEs) of Al 2p in Al-N and Al-O are 73.5 ± 0.3 eV and 74.5 ± 0.4 eV, respectively [26]. By deconvolution of the peak, we obtained BE of Al-N and Al-O were 73.5 and 74.3–74.9 eV at 274, 307, and 335 °C of $T_{dep}$. It should be noted that as the $T_{dep}$ increases from 274° to 335°C, the intensity of Al-N bonding state increases while that of Al-O decreases significantly.

The XPS spectra of N 1 s from AlN film grown at 274, 307 and 335 °C are shown in Fig. 6(b), (d) and (f). The reported BE of N-Al and N-Al-O are 396.4 ± 0.3 eV and 398.0 ± 0.3 eV, respectively [25]. We observed the BE of N-Al and N-Al-O are 396.4 eV and 397.0–398.0 eV at 274, 307, and 335 °C of $T_{dep}$. As $T_{dep}$ increases, the intensity of N-Al-O peak concurrently decreased. Both Al 2p and N 1 s spectra revealed that the amount of oxygen decreased as $T_d$ increased and this is consistent with the results obtained from AES analysis.

Table 1 shows the atomic concentrations of Al, N and O in the film calculated from the peak area of XPS spectra. The absolute values of atomic concentrations in AlN film obtained from XPS analysis is quite different from AES depth profile because both analysis were not calibrated by standard sample. However, we observed that in both methods oxygen concentration decreased by similar amount upon increasing $T_{dep}$ from 274° to 335°C.

The electrical properties of AlN films were studied by fabricating the devices having Al/AlN/Pt stack and DC *I-V* measurement as shown in Fig. 2. The thickness of AlN film was 8.9, 16.5, and 14.9 nm grown at 274, 307, and 335 °C, respectively. Due to the different film thickness, *J-E* curves were presented in Fig. 7(a) as log-linear scale. The electrical properties of the devices showed bias polarity, but it was possible to identify the different behavior between the low and the high field regions when positive bias voltage was applied. Their boundary was set to + 1.5 MV/cm because the change of current conduction occurred around this electric field.

In the low electric field (< 1.5 MV/cm) region, the device with $T_{dep}$ = 274 °C showed higher leakage current under positive bias voltage, while the device with $T_{dep}$ = 307 and 335 °C exhibited lower current value under both bias polarities. Such a polarity dependency of the device with $T_{dep}$ = 274 °C was attributed to the interface-limited conduction. Generally speaking, current (electron) injection could be limited at the metal/dielectric interface with higher work function of Pt (~ 5.6 eV) electrode compared to that of Al (~ 4.2 eV) counter electrode. However, this was not the case. Fluent current injection was observed in the device with $T_{dep}$ = 274 °C in the low field region under positive bias. This could be understood by the barrier inhomogeneity due to the interfacial defects owing to the low $T_{dep}$ [25,27]. Meanwhile, the device with $T_{dep}$ = 335 °C showed similar current values under positive and negative bias, which means that bulk-limited conduction becomes dominant. That is, the leakage current could be limited by the energy level of trap sites inside the film rather than the metal/dielectric

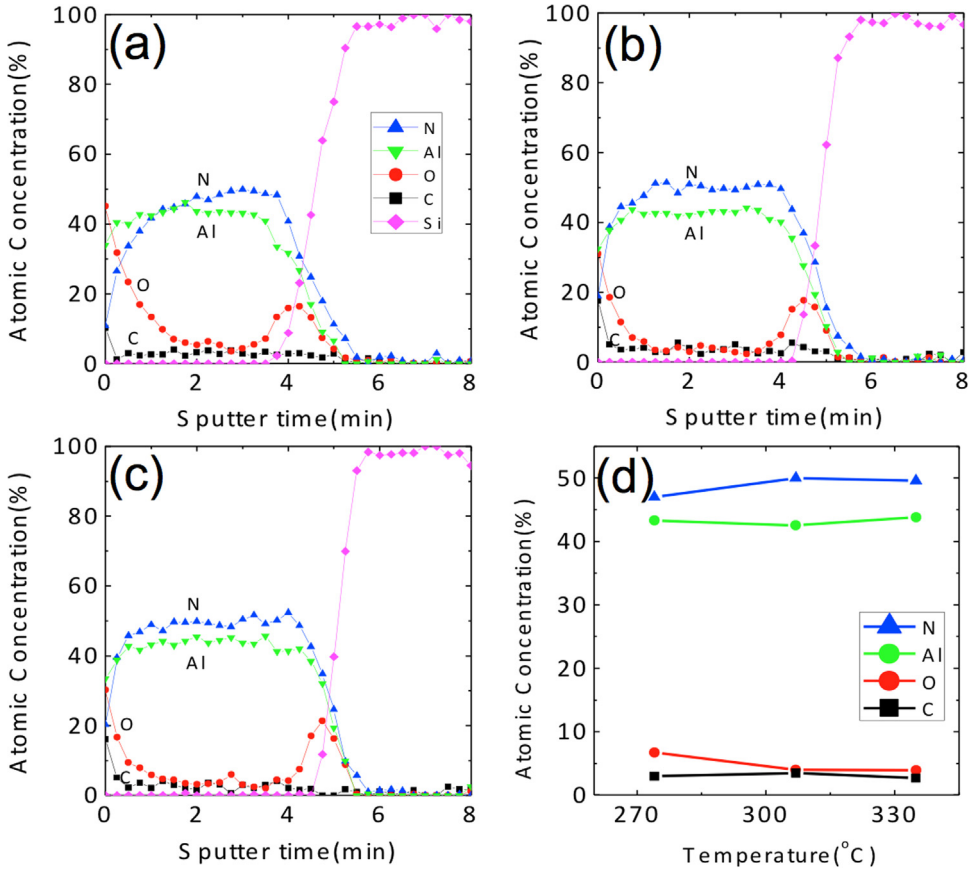


**Fig. 5.** AES depth profiles of elements in AlN thin films grown at (a) 274 °C, (b) 307 °C, and (c) 335 °C; (d) shows the average concentrations of Al, N, O and C as a function of growth temperature.

interface.

In the high electric field (> 1.5 MV/cm) region, inflection of the current level was observed especially under positive bias. Even lower leakage current was exhibited in the device with $T_{dep}$ = 274 °C than that of the device with $T_{dep}$ = 307 °C. The lowest current level was maintained in the device with $T_{dep}$ = 335 °C. To understand the current conduction in the devices, J-E curves were fitted with the formula of Poole-Frenkel emission model. Fig. 7(b) shows the result for Poole-Frenkel emission, this is the result of applying several carrier transport models to verify the conduction mechanism.

$$J = E \exp\left(\frac{-q(\phi_T - \sqrt{qE/(\pi\varepsilon_0\varepsilon_r)})}{k_B T}\right) \quad (1)$$

Where, J is the current density, E is the applied electric field, q is the elementary charge, $\phi_T$ is the trap barrier height (in zero applied electric field) that an electron must cross to move from one atom to another in the site, $\varepsilon_r$ is the dielectric constant, $k_B$ is Boltzmann's constant and $T$ is the temperature.

By fitting with the model, dielectric constant ($\varepsilon_r$) and trap barrier height ($\phi_T$) in the film were obtained from the slopes and y-axis intercept values as noted in Table 2. As the $T_{dep}$ increases, the dielectric constant slightly decreases, while the trap barrier height increases. The decrease in dielectric constant could be understood from the reduction of oxygen concentration. Dielectric constant of $Al_2O_3$ is 7.6, which value is higher than that of AlN ($\varepsilon_r$ = 4.48) [28–31]. Crystallization may also influence the dielectric constant, where dielectric constant slightly increases in the device with $T_{dep}$ = 335 °C compared to $T_{dep}$ = 307 °C. It is known that the crystallization of AlN may cause the increase in the dielectric constant [30].

Next, the increase in trap barrier height could be explained by the change of trap site. Two kinds of point defect are energetically favorable in AlN film; substitutional oxygen for nitrogen ($O_N$) and aluminum vacancy ($V_{Al}$) [31,32]. Their energy levels are ~ 0.8 eV for $O_N$ and ~ 1 eV for $V_{Al}$. Consequently, the increase in the trap barrier height can be understood from the decrease of the amount of $O_N$ and the increase of $V_{Al}$ with increasing $T_{dep}$, resulting in the change of the leakage current for the devices. The increase in the trap barrier height could be understood from the characteristics of O concentration and N-rich film as increasing $T_{dep}$.

## 4. Conclusion

Effect of Temperature on the growth of AlN film by thermal ALD using TMA as a metal precursor and $NH_3$ as a reaction gas was investigated. Structural, chemical and electrical properties of AlN film were studied in the temperature range of 274–335 °C. Film thickness was successfully controlled by the number of ALD cycles under self-limited growth condition. The growth rate increased from 0.05 to 0.16 nm/cycle upon increasing $T_{dep}$ from 274° to 335°C. The activation energy for the reaction of TMA with $NH_3$ was obtained (55 KJ/mol) from the Arrhenius plot. By increasing the growth temperature, the crystallinity of AlN thin films increased (polycrystalline hexagonal structure of wurtzite). AES analysis revealed that in AlN films the elemental concentration of oxygen was uniformly distributed. The oxygen concentration in the bulk of AlN thin films decreased upon increasing $T_{dep}$. XPS confirmed this - the intensity of the O 1 s peak decreased upon increasing $T_{dep}$. The chemical bonding states for AlN film, as determined by XPS, are Al-N and N-Al-O. *J-E* curve for the devices having Al/AlN/Pt stack with difference $T_{dep}$ were obtained to study the electrical properties of AlN films. It was confirmed that the devices were well fitted with Poole-Frenkel emission model under positive bias

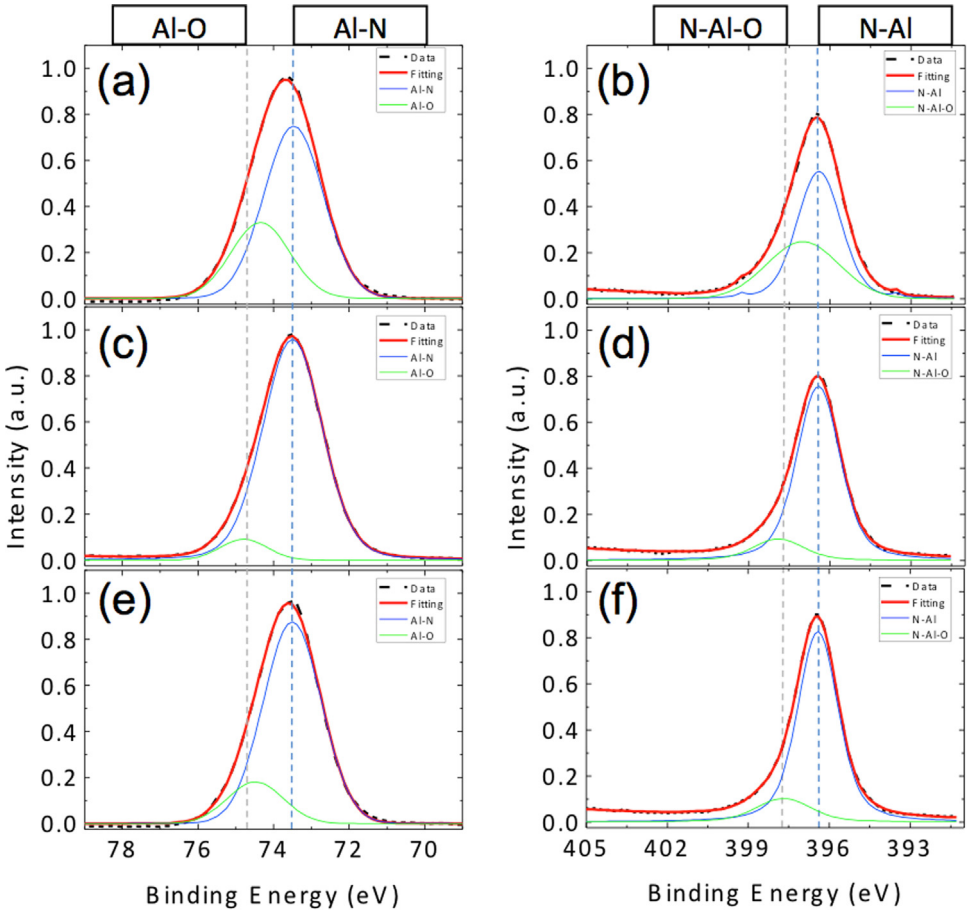


**Fig. 6.** XPS spectra of AlN thin films grown at (a)(b) 274 °C, (c)(d) 307 °C, (e)(f) 335 °C. (a), (c) and (e) shows Al 2p, and (b), (d) and (f) shows N 1s spectra, respectively.

**Table 1**
Average concentration of elements in AlN thin films verified by the Al2s, N1s and O1s XP spectra at the specified growth temperatures.

| $T_{dep}$ (°C) | Al (at%) | N (at%) | O (at%) |
|---|---|---|---|
| 274 | 47 | 30 | 23 |
| 307 | 50 | 32 | 18 |
| 335 | 48 | 36 | 16 |

**Table 2**
Fitting parameters for Poole-Frenkel emission, where dielectric constant ($\varepsilon_r$) and trap barrier height ($\phi_T$) were obtained from the slopes and y-axis intercept values, respectively.

| Forward bias | | |
|---|---|---|
| $T_{dep}$ (°C) | Dielectric constant ($\varepsilon_r$) | Trap barrier height ($\phi_T$) (eV) |
| 274 | 5.76 | 0.886 |
| 307 | 3.18 | 1.048 |
| 335 | 4.36 | 1.082 |

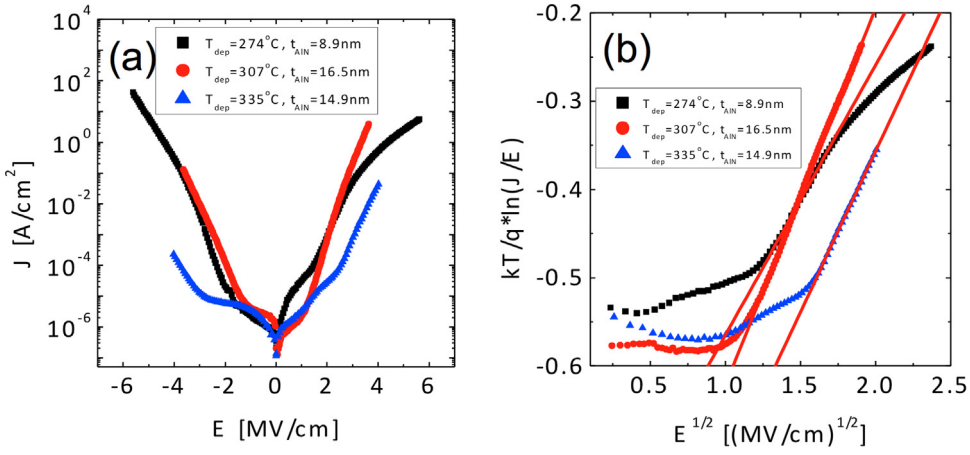


**Fig. 7.** Electrical property of AlN thin films deposited at 274 °C, 307 °C and 335 °C. (a) log *J-E* curves, (b) the fitting result for Poole-Frenkel emission model.

voltage on top of Al contact. The results have shown that the dielectric constant of the film decreased, while the trap barrier height increased upon increasing $T_{dep}$. $O_N$ and $V_{Al}$ were considered as feasible point defects consistent with the oxygen content and nonstoichiometry of the film.

## Acknowledgment

This research was supported by Basic Science Research Program through the National Research Foundation of Korea(NRF) funded by the Ministry of Education(2017R1D1A1A09000809).

## References

[1] Z.L. Tseng, L.C. Chen, W.Y. Li, S.Y. Chu, Resistive switching characteristics of sputtered AlN thin films, Ceram. Int. 42 (2016) 9496–9503.
[2] B.J. Choi, A.C. Torrezan, J.P. Strachan, P.G. Kotula, A.J. Lohn, M.J. Marinella, Z. Li, R.S. Williams, J.J. Yang, High-speed and low-energy nitride memristors, Adv. Funct. Mater. 26 (2016) 5290–5296.
[3] S. Banerjee, A.A.I. Aarnink, R. Ktuijs, A.Y. Kovalgin, J. Schmitz, PEALD AlN: controlling growth and film crystallinity, Phys. Status Solidi 12 (7) (2015) 1036–1042.
[4] H.V. Bui, M.D. Nguyen, F.B. Wiggers, A.A.I. Aarnink, M.P. de Jong, A.Y. Kovalgin, Self-limiting growth and thickness- and temperature- dependence of optical constants of ALD aln thin films, ECS J. Solid State Sci. Technol. 3 (2014) 101–106.
[5] M. Bosund, T. Sajavaara, Properties of AlN grown by plasma enhanced atomic layer deposition, Appl. Surf. Sci. 257 (2011) 7827–7830.
[6] M. Bosund, P. Mattila, A. Aierken, T. Hakkarainen, H. Koskenvaara, M. Sopanen, V.M. Airaksinen, H. Lipsanen, GaAs surface passivation by plasma-enhanced atomic-layer-deposited aluminum nitride, Appl. Surf. Sci. 256 (2010) 7434–7437.
[7] M. Usman, A. Hallen, T. Pilvi, A. Schoner, M. Leskela, Toward the understanding of stacked Al-based high-*k* dielectrics for passivation of 4H-SiC devices, J. Electrochem. Soc. 158 (2011) 75–79.
[8] H. Kim, D.H. Kim, B.J. Choi, Interfacial and electrical properties of $Al_2O_3$/GaN metal–oxide–semiconductor junctions with ultrathin AlN layer, Appl. Phys. A 123 (2017) 800.
[9] H.C. Seo, I. Petrov, K. Kim, Structural properties of AlN grown on sapphire at plasma self-heating conditions using reactive magnetron sputter deposition, J. Electron. Mater. 39 (2010) 1146–1151.
[10] H.Y. Joo, H.J. Kim, S.J. Kim, S.Y. Kim, Spectrophotometric analysis of aluminum nitride thin films, J. Vac. Sci. Technol. A 17 (1999) 862–870.
[11] J.M. Khoshman, M.E. Kordesch, Optical characterization of sputtered amorphous aluminum nitride thin films by spectroscopic ellipsometry, J. Non-Cryst. Solids 351 (2005) 3334–3340.
[12] H. Nomura, S. Meikle, Y. Nakanishi, Y. Hatanaka, Properties of AlN grown by plasma enhanced atomic layer deposition, J. Appl. Phys. 69 (2009) 990–993.
[13] K.S. Stevens, A. Ohtani, M. Kinniburgh, R. Beresford, Structural and mechanical characteristics of (103)/kiN thin films prepared by radio frequency magnetron sputtering, Appl. Phys. Lett. 65 (2009) 321–323.
[14] S. Goerke, M. Ziegler, A. Ihring, J. Dellith, A. Undisz, M. Diegel, S. Anders, U. Huebner, M. Rettenmayr, H.G. Meyer, Atomic layer deposition of aln for thin membranes using trimethylaluminum and H2/N2 plasma, Appl. Surf. Sci. 338 (2015) 35–41.
[15] Y.J. Lee, S.W. Kang, Growth of aluminum nitride thin films prepared by plasma-enhanced atomic layer deposition, Thin Solid Films 446 (2004) 227–231.
[16] C. Ozgit, I. Donmez, M. Alevli, N. Biyikli, Self-limiting low-temperature growth of crystalline AlN thin films by plasma-enhanced atomic layer deposition, Thin Solid Films 520 (2012) 2750–2755.
[17] M. Alevli, C. Ozgit, I. Donmez, The influence of growth temperature on the properties of AlN films grown by atomic layer deposition, Acta Phys. Pol. 120 (2011) 19–23.
[18] J. Dendooven, D. Deduytsche, J. Musschoot, R.L. Vanmeirhaeghe, C. Detavernier, Conformality of Al2O3 and AlN deposited by plasma-enhanced atomic layer deposition, J. Electrochem. Soc. 157 (2010) 1111–1116.
[19] Y.J. Lee, Formation of aluminum nitride thin films as gate dielectrics on Si (1 0 0), J. Cryst. Growth 266 (2004) 568–572.
[20] X. Liu, S. Ramanathan, E. Lee, T.E. Seidel, Atomic layer deposition of aluminum nitride thin films from trimethyl aluminum (TMA) and ammonia, MRS Proceedings, Cambridge Univ Press, 811, 2004.
[21] K.H. Kim, N.W. Kwak, S.H. Lee, Fabrication and properties of A1N film on gan substrate by using remote plasma atomic layer deposition method, Electr. Mater. Lett. 5 (2009) 83–86.
[22] R.L. Puurunen, Surface chemistry of atomic layer deposition: a case study for the trimethylaluminum/water process, J. Appl. Phys. 97 (2005) 121301.
[23] B.J. Choi, J.J. Yang, M.X. Zhang, K.J. Norris, D.A.A. Ohlberg, N.P. Kobayashi, G.M. Ribeiro, R.S. Williams, Nitride memristors, Appl. Phys. A 109 (2012) 1–4.
[24] P. Motamedi, K. Cadien, XPS analysis of AlN thin films deposited by plasma enhanced atomic layer deposition, Appl. Surf. Sci. 315 (2014) 104–109.
[25] L. Rosenberger, R. Baird, E. McCullen, G. Auner, G. Shreve, XPS analysis of aluminum nitride films deposited by plasma source molecular beam epitaxy, Surf. Inter. Anal. 40 (2008) 1254–1261.
[26] Z. An, C. Men, Z. Xu, P.K. Chu, C. Lin, Electrical properties of AlN thin films prepared by ion beam enhanced deposition, Surf. Coat. Technol. 196 (2005) 130–134.
[27] H. Morkoc, T.J. Drummond, R. Fischer, Interfacial properties of (Al, Ga) As/GaAs structures: effect of substrate temperature during growth by molecular beam epitaxy, J. Appl. Phys. 53 (1982) 1030–1033.
[28] S. Saib, N. Bouarissa, P. Rodríguez-Hernández, A. Muñoz, Structural and dielectric properties of AlN under pressure, Phys. B 403 (2008) 4059–4062.
[29] M.D. Groner, J.W. Elam, F.H. Fabreguette, S.M. George, Electrical characterization of thin Al2O3 films grown by atomic layer deposition on silicon and various metal substrates, Thin Solid Films 413 (2002) 186–197.
[30] S. Jakschik, U. Schroeder, T. Hecht, M. Gutsche, H. Seidl, J.W. Bartha, Crystallization behavior of thin ALD-Al2O3 films, Thin Solid Films 425 (2003) 216–220.
[31] C. Stampfl, C.G. van de Walle, Theoretical investigation of native defects, impurities, and complexes in aluminum nitride, Phys. Rev. B. 65 (2002) 1–9.
[32] M. Bickermann, B.M. Epelbaum, O. Filip, P. Heimann, S. Nagata, A. Winnacker, Point defect content and optical transitions in bulk aluminum nitride crystals, Phys. Status Solidi B 246 (2009) 1181–1183.